Valorization of Mexican biomasses through pyrolysis, combustion and gasification processes

M.M. Parascanu[a], F. Sandoval-Salas[b], G. Soreanu[c], J.L. Valverde[a], L. Sanchez-Silva[a,*]

[a] *University of Castilla-La Mancha, Department of Chemical Engineering, Avda. Camilo José Cela, 12, 13071 Ciudad Real, Spain*
[b] *Instituto Tecnológico Superior de Perote, Carretera Federal Perote-México Km. 2.5, 91270 Perote, Mexico*
[c] *Technical University "Gheorghe Asachi" of Iasi, Department of Environmental Engineering and Management, 73 D. Mangeron Blvd, 700050 Iasi, Romania*

ARTICLE INFO

ABSTRACT

Pyrolysis, combustion and gasification processes of six different types of biomass, which were obtained from Mexico (Castor husk, Castor stem, *Agave* bagasse, Coffee pulp, *Opuntia* stem and *Pinus* sawdust) were investigated by means of thermogravimetric analysis coupled with mass spectrometry (TG-MS). The selection of biomass, for each thermochemical process, depended on its main physico-chemical properties (moisture content, volatile matter, fixed carbon, ash content, calorific value, mineral content, etc.). For pyrolysis processes, the desirable characteristics of biomass are high volatile matter and low ash content. For combustion processes, the biomass has to show high low heating value (LHV) and low ash content. In the case of gasification processes, the biomass ought to have high fixed carbon. *Pinus* sawdust had the highest volatile matter and the lowest ash content, Castor stem showed the highest LHV and Coffee pulp had the highest fixed carbon content. The pyrolysis process was divided in three main stages (dehydration, devolatilization and char formation). Moreover, for *Agave* bagasse two more peaks at high temperature were found due to the decomposition of lignin and cellulose but it could also be related to its high mineral content. On the other hand, three main different stages (dehydration, devolatilization and char oxidation) for the combustion process were found. It is noticeable that Coffee pulp showed one more peak than other studied biomasses, which is related to its high lignin content. Due to its high heat released, Castor husk could be considered as the best candidate for combustion process. However, *Pinus* sawdust can be considerate more suitable for this process because of its low amount of NO_x released. In addition, for gasification process the effect of the gas flow was studied. Coffee pulp resulted to be the most suitable for gasification process due to the amount and quality of the fuel gas produced.

1. Introduction

As a result of population growth, a worldwide energy demand increase is expected in the future. This situation, combined with the gradual depletion of fossil fuels and the environmental problems associated with their use, has motivated the search of new alternatives for keeping a sustainable energy production [1,2]. In this sense, biomass could be a possible substitute since it could satisfy part of the future energy demand in a sustainable manner [3,4].

Particularly, biomass is considered a viable option for energy production in Mexico [5] because a lot of agricultural products and agroindustrial wastes are annually generated. The choice of raw materials that should be used in large-scale energy production processes depends on their physico-chemical properties and its availability. In general, it is assumed as a requirement that their production do not compete with food crops for lands and water resources. In addition, the potential of a negative impact of the use of each biomass on the environment should be considered [6].

Among the biomass with the highest potential for energy production are the plants from *Agave* and *Opuntia* genera. Some species of these genera are native of America and widely grown in Mexico. Due to their metabolism, those, having a Crassulacean Acid Metabolism (CAM), have high efficiencies of water use (five or ten times higher than plants C_3 and C_4) and are suitable to grow in environments with limitations, such as arid regions and marginal soils [7,8]. Moreover, these species are also highly efficient in biomass accumulation. It has been estimated that an *Agave* crop can yield from 10 to 34 t/ha per year. These values exceed those obtained with switchgrass (15 t/ha per year) and poplar (11 t/ha per year) [9]. Moreover, under irrigation conditions yields comparable with cane sugar can be obtained [10].

---

* Corresponding author.
E-mail address: marialuz.sanchez@uclm.es (L. Sanchez-Silva).

On the other hand, the coffee processing industry generates a lot of pulp. This waste is usually disposed of in nearby land and water bodies causing serious environmental problems. Additionally, the presence of toxic compounds such as caffeine, phenols and tannins makes the use of this material difficult [11–14]. Due to the high content of lignocellulose and sugars in the pulp coffee [4,15,16], high yields can be expected in the use of this biomass for the energy production, thus limiting environmental problems caused by improper disposal of this material. Moreover, possibilities of bioethanol production from coffee pulp in a sustainable manner was investigated [17]. Pandey et al. [18] studied the possibility of using coffee pulp as animal feed, but the caffeine and tannins content present in coffee pulp was demonstrated to affect the animal health [18], thus, its use as soil fertilizer was recommended [19].

Other biomass with high potential for the energy production in Mexico is the pine sawdust. About 280,000 t of this material are yearly produced. Its high specific energy (17–21 MJ/Kg) [20] allows that a small part could be used as fuel for drying in sawmills.

An increasing attention to the Castor oil production has been paid in the last years, since it is considered an excellent raw material for the chemical and biofuel production industries [21]. Large amounts of cake, husk and crop residues are obtained as by-products of the Castor oil extraction [22]. The cake from Castor oil extraction can be used for different purposes: fertilizer [23], enzyme production [24–26], bioethanol production [27] and biogas production [28]. However, despite of the large amount of husk generated, few works focused on its further use have been reported.

Biomass can be exploited directly or through thermochemical or biochemical processes to obtain electrical, thermal or chemical energy. The main biochemical processes are alcoholic fermentation and anaerobic digestion that usually yield bioethanol and biogas, respectively [29–31].

Thermochemical conversion processes include three basis subcategories: combustion, pyrolysis/liquefaction and gasification [32]. Combustion and pyrolysis of biomass are regarded as the most widely used conversion processes of biomass for energy and has been investigated for a long time [33]. Combustion can be defined as the conversion of biomass, in contact with air or oxygen, to several forms of useful energy [34]. However, pyrolysis is a process of producing gas, oil and solid from biomass using high temperature in the absence of air or steam. The conventional gasification technology can be defined as the partial combustion of biomass by controlling the amount of air to transform hydrocarbons into carbon monoxide, carbon dioxide and hydrogen. Gasification studies have been reported in literature, being most of them focused on the use of coal [35–39].

Biomass thermochemical conversion can be investigated by thermogravimetric techniques (TGA). The main advantages of TGA are accurate real-time data on the basis of the directly measured mass of the sample, high reproducibility, well-defined temperature and gas phase conditions [40]. TGA technique has been previously used to characterize *Agave sisal* fibres [41,42] and *Agave tequilana* bagasse composition [43,44]. In addition, the pyrolysis of *Agave salmiana* bagasse has been also reported [45,46]. Furthermore, there are some works dealing with the pyrolysis of *Pinus cubensis* t [47] and *Pinus* sp. sawdust [48], and the combustion of *Pinus banksiana* and *Black spruce* mixtures [8]. However, there are few studies focused on the effect of the physical and chemical properties of Mexican waste biomass on the performance of pyrolysis, combustion and gasification processes.

In addition, different thermochemical processes (pyrolysis, combustion, torrefaction and gasification) of different type of microalgae were investigated in order to produce syngas and other products [29,30,49]. Moreover, co-pyrolysis of microalgae and sewage sludge was investigated to justify that this process is a promising way to fuel production [50]. In addition, TGA-FTIR-MS analysis of tobacco stem in inert atmosphere was carried out, pointing out its potential to be used

as a renewable feedstock [51]. An oxidative fast pyrolysis in an autothermal fluidized bed reactor of dried banana leaves has been also studied [52]. In addition, animal biomass such as dried manure was used as feedstock for pyrolysis, combustion and gasification [53–57]. Furthermore, activated sludge was also used as a precursor for the production of activated carbon using sulfuric acid as a chemical activation agent [58]. Activated carbon can be obtained using a wide range of biomass as coconut residue [59], coal and derivative agricultural products or lignocellulosic materials [60].

The current low level of utilization of agricultural waste biomass as fuel is attributed to the lack of proper information concerning their properties such as moisture content, bulk density, melting point of the ash and content of volatile matter [61].

The aim of this work was to study the thermal behaviour of different types of Mexican biomass through pyrolysis, combustion and gasification processes. Firstly, all studied biomasses were characterized by proximate and ultimate analyses, Inductively Coupled Plasma Spectrometry (ICP), bomb calorimetry and pycnometry in order to determine their main physical-chemical properties. Following the characterization results obtained, a number of biomass samples were selected for the pyrolysis, combustion and gasification experiments. In addition, gases released were analyzed by a mass spectrometer and the effect of O_2 concentration in the gasification process was evaluated.

2. Materials and methods (Experimental)

2.1. Materials

Castor stems (*Ricinus communis*) was collected from crops established in Veracruz (Mexico) and castor husk was obtained after castor capsules threshing process. *Opuntia* (*Opuntia ficus-indica*) was collected from crops established in Veracruz. *Agave* bagasse was extracted from a juice coming from fresh leaves of *Agave salmiana* using a hammer mill. Coffee pulp (comprising the skin and mesocarp of the berry of *Coffea arabica*) and *Pinus* sawdust (*Pinus patula*) were obtained from coffee wet processing and wood sawmill, respectively. Coffee pulp and *Agave* bagasse were predried for 2 days under solar radiation. Subsequently, samples were dried in an oven at 70 °C for 24 h in order to facilitate their transportation. All biomasses were milled and sieved to an average particle size ranging from 100 to 150 μm.

2.2. Equipment and procedures for biomass characterization

The evaluation of biomass composition was carried out by proximate analysis to measure the volatile matter, fixed carbon and ash content according to a study published elsewhere [62]. The ultimate analysis was used to determine the concentration of carbon, hydrogen, nitrogen, oxygen and sulphur content of a sample. The determination of the higher heating values (HHV) was made according to the standard UNE-EN 14918 using a bomb calorimeter PARR 1356. The lower heating value (LHV) was estimated from the higher heating value (HHV) considering the content of hydrogen and moisture in the biomass [63]. Mineral composition of biomass was measured by using Inductively Coupled Plasma Spectrometer (model Liberty Sequential Varian) [49].

The density of biomass samples was determined by using an Ultrapyc 1200e gas pycnometer (Quantachrome Instruments Co., Ltd.) that allowed to measure up to 135 cm^3 of sample volume. The advantage of this equipment is that calculation of results were fully automatic. Samples were analyzed as many times as needed to obtain an accurate measurement. To determine the bulk density of the biomass, a standard sample cell was employed whereas nitrogen was used as the carrier gas.

Phenom ProX desktop scanning electron microscope (SEM) was used to evaluate the morphology and structure of the biomass particle.

Table 1

Characterization of Castor husk, Castor stems, *Agave* bagasse, Coffee pulp, *Opuntia* stem and *Pinus* sawdust.

	Ultimate analysis (wt%)					Proximate analysis (wt%)			
	C	H	N	S	O[*diff]	Moisture	Ash	Volatile matter	Fixed carbon[*diff]
Castor husk	46.21	6.03	2.03	0.35	45.38	3.45	3.60	74.13	18.82
Castor stem	46.47	5.94	0.89	0.36	46.34	4.27	1.70	78.01	16.03
Agave bagasse	39.81	5.08	1.79	0.30	53.02	2.68	11.41	71.00	14.90
Coffee pulp	43.33	5.69	2.50	0.35	48.13	2.74	6.55	69.48	21.23
Opuntia stem	34.72	5.07	4.32	0.03	55.86	1.57	15.32	66.78	16.33
Pinus sawdust	48.99	6.72	0.35	0.03	43.91	3.41	1.30	80.15	15.14
	Mineral content (ppm)					Bomb calorimeter (MJ/kg)			
	Ca	Cl	P	K	Mg	LHV	HHV		Density (kg/m^3)
Castor husk	1675	223,439	3046	–	–	16.48	17.79		1511.2
Castor stem	239	229,998	1386	–	–	17.68	18.97		1726.7
Agave bagasse	60,295	125,829	509	5593	5865	14.10	15.43		1650.0
Coffee pulp	2716	177,159	1363	–	–	14.95	16.28		1512.1
Opuntia stem	39,319	31321	5101	4745	8369	11.68	12.73		1629.2
Pinus sawdust	–	85740	730	–	–	16.32	17.70		1346.3

O[*diff]: obtained by difference of C, H, N, S and Ash; Fixed carbon[*diff]: calculated from the difference of Moisture, Ash and Volatile Matter.
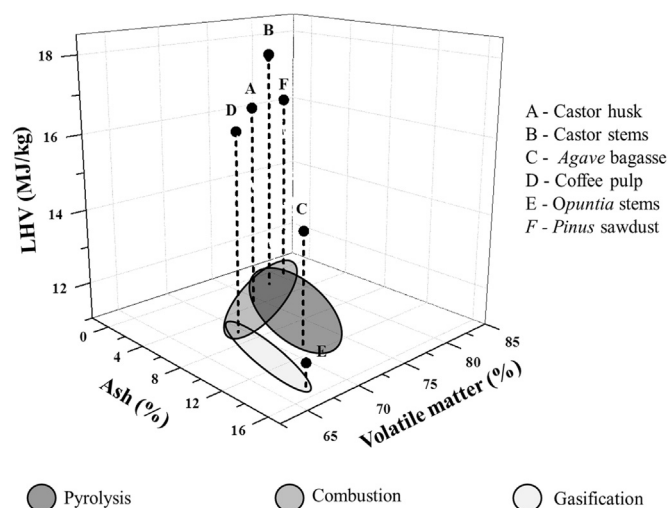

Fig. 1. 3D diagram description low heating value (LHV), ash content (wt%) and volatile matter (wt%) of six Mexican biomasses (Castor husk, Castor stems, *Agave* bagasse, Coffee pulp, *Opuntia* stems, *Pinus* sawdust).

Infrared spectra (FTIR) were obtained from a Spectrum Two spectrometer (Perkin Elmer, Inc.) having a universal attenuated total reflectance accessory (UATR). The spectral range considered ranged from 4000 to 450 cm^{-1} at resolution of 4 cm^{-1}. A small amount of a sample was placed over the cell and carefully pressed until the transmittance signal was stabilized. All determinations were performed at room temperature.

Table 1 shows the results of ultimate and proximate analyses, mineral content, higher and lower heating values, and bulk density for the samples of Castor husk, Castor stem, *Agave* bagasse, Coffee pulp, *Opuntia* stem and *Pinus* sawdust.

2.3. Thermogravimetric analysis coupled to Mass Spectrometer (MS)

The thermochemical conversion processes of biomasses was carried out in a Mettler-Toledo TGA apparatus (TGA–DSC) coupled to a mass spectrometer (Thermostar-GSD 320/quadrupole mass analyser; Pfeiffer Vacuum) with an electron ionization voltage at 70 eV and provided mass spectra up to 300 a.m.u. A semiquantitative analysis was performed by using a normalization procedure. The weight of the samples were fixed at 8 mg. Pyrolysis experiments were performed from 25 to 1000 °C at a heating rate of 10 °C/min and under constant

flow of 200 N ml/min of Argon in order to ensure inert conditions. Combustion experiments were performed from 25 to 800 °C (heating rate of 10 °C/min) under a reactive atmosphere of 100 N ml/min of O_2/Ar (21 vol%/79 vol%). Regarding the gasification process. the selected biomass samples (Coffee pulp and *Opuntia* stem) were firstly pyrolyzed in a tubular reactor under a continuous N2 flow of 200 Nml/min from room temperature to 900 °C with a 10 °C/min heating rate and kept around 900 °C for 1 h with the aim to obtain the char used in the gasification process. The gasification stage was performed in two steps. The first one was performed from 25 to 900 °C at a heating rate of 40 °C/min under an Ar flow of 200 N ml/min, then being kept at 900 °C for 5 min. In the second step, samples were kept at 900 °C for 1 h using a flow 50 Nml/min of a gas mixture constituted by Ar and O2. To determine the optimal proportion of O2 in the mixture, different experiments were carried out by varying the ratio Ar/O2 (vol%/vol%) at 95/5, 90/10, 85/15 and 79/21.

3. Results and discussion

3.1. Selection of biomass

The main physicochemical characteristics of the different biomasses used in this study [64]: moisture content, volatile matter, fixed carbon, ash content, calorific value, mineral content and cellulose/lignin ratio, are listed in Table 1. In addition, Fig. 1 shows a tridimensional diagram where the low heating value (LHV, MJ/kg), ash content (wt%) and volatile matter (wt%) of all the samples are considered as axes. Regarding the pyrolysis process, the biomass ought to have a high volatile matter whereas the ash content should be low [64]. In this context, Castor husk, Castor stem, *Agave* bagasse and *Pinus* sawdust samples were selected for the pyrolysis study (Fig. 1). Regarding the combustion process, the most important parameter to be considered is the heating value [65] which is influenced by the carbon, hydrogen and oxygen concentrations in the biomass. Consequently, the biomass is to have a high HHV/LHV ratio and led to a low ash content. In this context, Castor husk, Castor stem, Coffee pulp and *Pinus* sawdust were selected for the combustion study. Regarding the gasification process, the biomass ought to have high fixed carbon (Table 1) and low ash content [64]. Therefore, Coffee pulp and *Opuntia* stem samples were selected due to their high fixed carbon content. On the other hand, ash content of biomass should be low since it has an impact on the total cost of the thermochemical process [62]. In addition, biomass density has also an impact on the behaviour of thermochemical conversion processes; thus dense particles contribute to a longer burnout time. On
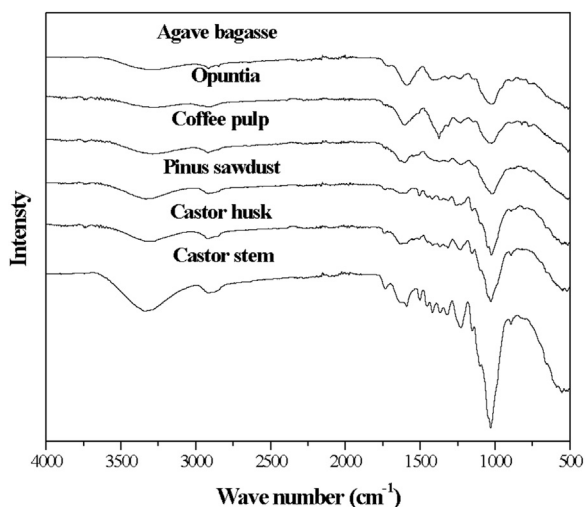
Fig. 2. FTIR spectra of: Castor husk, Castor stems, *Agave* bagasse, Coffee pulp, *Opuntia* stems, *Pinus* sawdust.
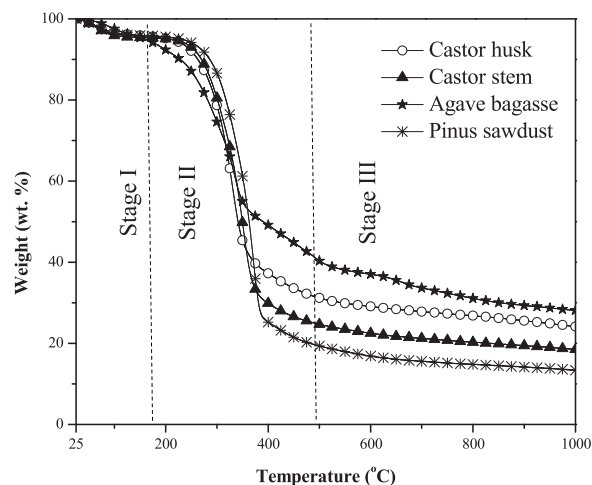

Fig. 3. Thermogravimetric (TGA) curves of the pyrolysis process of the biomass simple studied: Castor husk, Castor stems, *Agave* bagasse, *Pinus* sawdust.

the contrary, low biomass density not only yields to a low energy density but also leads to high transportation costs and reduces the storage capacity of both the biomass producer and the end-user [66]. Table 1 shows small differences in the density values of the different biomasses (Pinus sawdust was the one with lowest density whereas Castor stem was the one with the highest density).

Fig. 2 shows the FTIR spectra of Castor husk, Castor stem, *Agave* bagasse, Coffee pulp, *Opuntia* stem and *Pinus* sawdust. This technique was used to determine the presence of functional groups such as alkenes, esters, aromatics, ketones and alcohols in a particular biomass [67]. The main bands were related to the presence of hemicellulose, cellulose and lignin, which are the main components of a biomass. Lignin is a biopolymer material built up from the phenyl propane nucleus, an aromatic ring with a three-carbon side chain, vanillin, syringaldehyde and tannins (complex polyhydric phenols) [68].

For all the studied biomasses, the peak in the region between 3600 cm^{-1} and 3000 cm^{-1} corresponded to the stretching vibration of OH due to the presence of cellulose and lignin. The peak in the region between 3000 and 2700 cm^{-1} was related to the stretching vibration of CH [69]. The peak observed around 1650 cm^{-1} was attributed to the $C=O$ bond in hemicellulose. The peak detected in the region from 1440 cm^{-1} and 1380 cm^{-1} corresponded to the asymmetric bending of the lignin structure [70]. *Opuntia* stem showed a different profile in this region which can be attributed to the presence of aromatic rings in lignin and *Opuntia* stem. Peaks near 1250 cm^{-1} can be related to the presence of C–O–C in the cellulose biopolymer chain [71]. In addition, all biomasses also showed an increase in the intensity of the band between 1100 cm^{-1} and 900 cm^{-1} region which was related to the C–O-H stretching vibration linkages in cellulose and hemicellulose or the presence of C–O–R alcohols or esters [70,71]. The additional peak around of 600 cm^{-1} can be associated to bending modes of aromatic compounds [72].

3.2. Pyrolysis process

Fig. 3 shows the thermogravimetric (TG) curves for the pyrolysis process of *Pinus* sawdust, Castor husk, Castor stems and *Agave* bagasse using a heating rate of 40 °C/min. Table 2 lists the most relevant pyrolytic characteristics of the samples studied, which are based on the derivative thermogravimetric (DTG) profile. T_{pyr} is the temperature at which the decomposition and weight loss of the sample starts took place. T_m represents the temperature at which a peak in the DTG curve starts to appear. Finally, the maximum weight loss rate $((dw/dT)_{max} \text{ (wt\%/°C)})$ of each peak can be also listed in Table 2.

The pyrolysis process took place in three decomposition stages. The first stage (I) occurred from 25 to 200 °C, which corresponded to a small mass loss due to dehydration and slight volatile release. The second one (II), ranging from 200 to 500 °C, was associated to the major mass loss, which was attributed to devolatilization, including release from biomass degradation. The third stage (III) took place from 500 to 1000 °C, and refers to the decomposition of remained biomass and char formation [49,73]. According to Zabeti et al. [74], the main weight loss was related to the decomposition of the main components of the biomass (cellulose, hemicellulose and lignin).

Pinus sawdust showed the highest pyrolysis temperature and the highest peak height at 370 °C (Table 2), which was mainly associated to cellulose decomposition. As described by Zabeti et al. [74], the degradation of cellulose takes place in a narrow temperature range (200–500 °C), where the mass loss occurs rapidly. Fig. 3 shows that Castor stem and Castor husk TGA profiles were similar to that of *Pinus* sawdust. It is associated with the degradation of the stable chains of hemicellulose and cellulose, producing volatiles [75]. However, the DTG profile (Table 2) shows that the *Pinus* sawdust decomposed faster than Castor stem and Castor husk. This fact can be assigned to the higher content of cellulose in the former [76].

On the other hand, *Agave* bagasse showed a different pyrolysis profile. It decomposed slower than others three ones, which could be associated to the slow decomposition of lignin [74]. Its pyrolysis profile showed four main peaks (Fig. 3, Table 2), the firsts two corresponded to dehydration and devolatilization processes, respectively. The two last peaks (3rd and 4th in Table 2) were related to the decomposition of lignin and cellulose by disintegration of monomeric phenols, aromatic rings and piranose structures present in their structures [77]. These peaks could also be related to the high mineral content in the samples, such as Ca, Mg and K, being 60,295, 5865 and 5593 ppm, respectively [78–80]. Moreover, the differences in the maximum weight loss rate (*Pinus* sawdust > Castor stem > Castor husk > *Agave* bagasse) can be related to the volatile matter content [76,81–83].

Finally, the residue yield of biomass pyrolysis for each type of biomass can be listed in Table 2. The residue from the pyrolysis can be associated with the ash content and fixed carbon (Table 1). In this sense, *Pinus* sawdust was the biomass with the lowest ash content and the highest fixed carbon (6.73 and 21.83 wt%, respectively). Consequently, *Pinus* sawdust residue from pyrolysis was the lowest one in value (13.36 wt%) if compared to that of Castor stem (18.52 wt %), Castor husk (24.13 wt%) and *Agave* bagasse (28.13 wt%).

The main products derived from the pyrolysis of the studied biomasses were evaluated by mass spectrometry (MS) analysis. The main ions released in the pyrolysis process were detected at $(m/z)=2$,

Table 2

Pyrolysis characteristics of *Pinus* sawdust, *Agave* bagasse, Castor husk and Castor stems.

Biomass sample	T_{pyr}[a] (°C)	T_m (°C)[b]				$(dw/dT)_{max}$ (wt%/°C)[c]				Residue yield (wt%)
		1st peak	2nd peak	3rd peak	4th peak	1st peak	2nd peak	3rd peak	4th peak	
Castor husk	167	64	330	–	–	0.07	0.83	–	–	24.13
Castor stem	190	62	352	–	–	0.09	0.95	–	–	18.52
***Agave* bagasse**	145	81	333	485	656	0.02	0.52	0.11	0.09	28.13
***Pinus* sawdust**	191	64	370	–	–	0.075	1.21	–	–	13.36

[a] Temperature at which pyrolysis started.
[b] Temperature at which a peak in the DTG curve was observed.
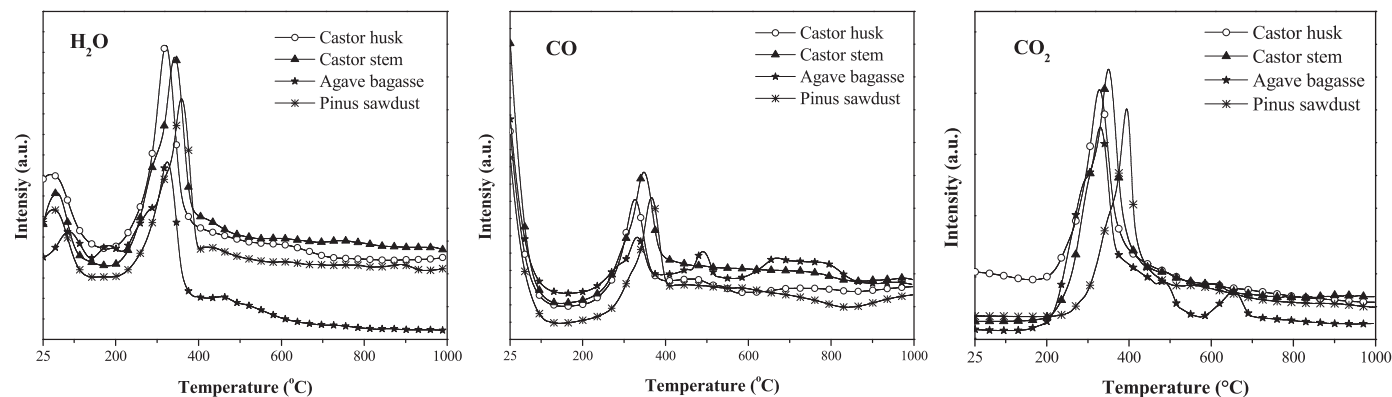[c] Maximum weight loss rate.

Fig. 4. Mass spectra of the pyrolysis process of Castor husk, Castor stems, *Agave* bagasse, *Pinus* sawdust for: H_2O, CO and CO_2.

15, 16, 18, 26, 27, 28, 29, 30, 41, 43, 44 and 78, which corresponded to the following compounds: H_2, CH_3^+, CH_4, H_2O, C_2H_2/CN, HCN/$C_2H_3^+$, CO, $C_2H_5^+$, C_2H_6, $C_3H_5^+$, $C_3H_7^+$, CO_2 and C_6H_6.

Figs. 4–6 shows the mass spectra coming from the pyrolysis of Castor husk, Castor stem, *Agave* bagasse and *Pinus* sawdust. During the pyrolysis process, H_2O, CO and CH_4 were observed at the beginning of process (< 150 °C), which was associated to the dehydration stage where the moisture and light volatiles components were loss. Most of the gas products (CH_3^+, CH_4, H_2O, C_2H_2/CN, HCN/$C_2H_3^+$, CO, $C_2H_5^+$, C_2H_6 $C_3H_5^+$, $C_3H_7^+$ and CO_2) were detected at the second stage, devolatilization stage (200–500 °C), due to the degradation of cellulose, hemicellulose and lignin. In the last stage (> 500 °C), CH_4, C_2H_2/CN, HCN/$C_2H_3^+$, CH_3^+, $C_3H_5^+$ and $C_3H_7^+$ were detected from the decomposition of the residue.

In all cases, the H_2 formation was detected at a temperature above 600 °C. This fact is probably caused by hydrocarbons (aromatics and aliphatics) thermal cracking and dehydrogenation ($C_nH_m \leftrightarrow C_{n-x}H_{m-y}+H_2+C+CH_4$). These reactions were probably catalyzed by the mineral content of biomass [84]. CH_4 concentration decreased at high temperatures due to its decomposition into char and H_2 [85]. The CO_2 formed at low temperatures can be due to the thermal decomposition of carboxylic groups by lignin degradation [86]. CO could be produced from the cracking of the carbonyl group, the rupture of heterocyclic oxygen and the dehydrogenation of hydroxyl group which is followed by the decomposition of hemicellulose [85,86]. HCN/$C_2H_3^+$ showed two peaks between 200–400 °C and 400–600 °C, respectively, coming from the decomposition of proteins which led to the release of volatile cyclic amides and HCN [87]. The hydrocarbons were formed in the main devolatilization stage, due probably to the occurrence of gas-phase secondary reactions and the decomposition of lipids [87].

Unlike Agave bagasse, Castor stem, Castor husk and *Pinus* sawdust presented similar MS spectrum profiles. The main differences were observed in the last stage (> 500 °C). The pyrolysis of Agave bagasse yielded the following species not detected in the pyrolysis of other biomasses: CO, CO_2, $C_2H_5^+$, C_2H_6, C_2H_2/CN, and C6H6. In addition, for *Agave* bagasse (whose composition is very different from that of the rest of biomasses, Table 1) the intensity of the peaks of the following species: H_2, CH_3^+, HCN/$C_2H_3^+$, $C_3H_5^+$ and CH_4, which were released in the pyrolysis of all the biomasses tested, was the highest one.

3.3. Combustion process

Fig. 7 shows the TGA curves for the combustion process of *Pinus* sawdust, Coffee pulp, Castor husk and Castor stem using a heating rate of 10 °C/min. Table 3 summarizes the main relevant combustion characteristics of samples studied, which are based on the derivative thermogravimetric (DTG) profile. T_{comb} is the temperature at which the decomposition and weight loss of the sample starts. T_m represents the temperature when a peak in the DTG curve starts to appear. Finally, the maximum weight loss rate ($(dw/dT)_{max}$ (wt%/°C)) for each peak can also be listed in Table 3.

The thermal degradation of biomass under oxygen atmosphere takes place in three main different stages [88–90]. The first stage can be attributed to the moisture loss and the highly volatile matters in the samples (25–125 °C). The second one, ranging from 125 °C to 350 °C, was characterized by the main mass loss which involved the oxidation degradation and the removal of the volatile matter of the samples. The last stage (350–525 °C) corresponded to the oxidation of the remaining char once volatiles were removed in the second stage. Generally, the second stage is attributed to the decomposition of hemicellulose and cellulose whereas the third stage is associated with the decomposition of lignin [8,87,91].

Coffee pulp started to decompose at the lowest temperature, 130 °C, (*Pinus* sawdust > Castor stem > Castor husk > Coffee pulp). However, the highest decomposition temperature was observed for *Pinus* sawdust (205 °C). This fact could be attributed to the volatile matter content in this biomass (Table 1). In this sense, *Pinus* sawdust presented the highest volatile matter content (80.15 wt%) followed by Castor stem (78.01 wt%) and Castor husk (74.13 wt%) whereas the Coffee pulp showed the lowest volatile matter content (69.48 wt%).

In addition, other differences can be observed in the combustion behaviour of the biomasses studied. Regarding the second decomposi-
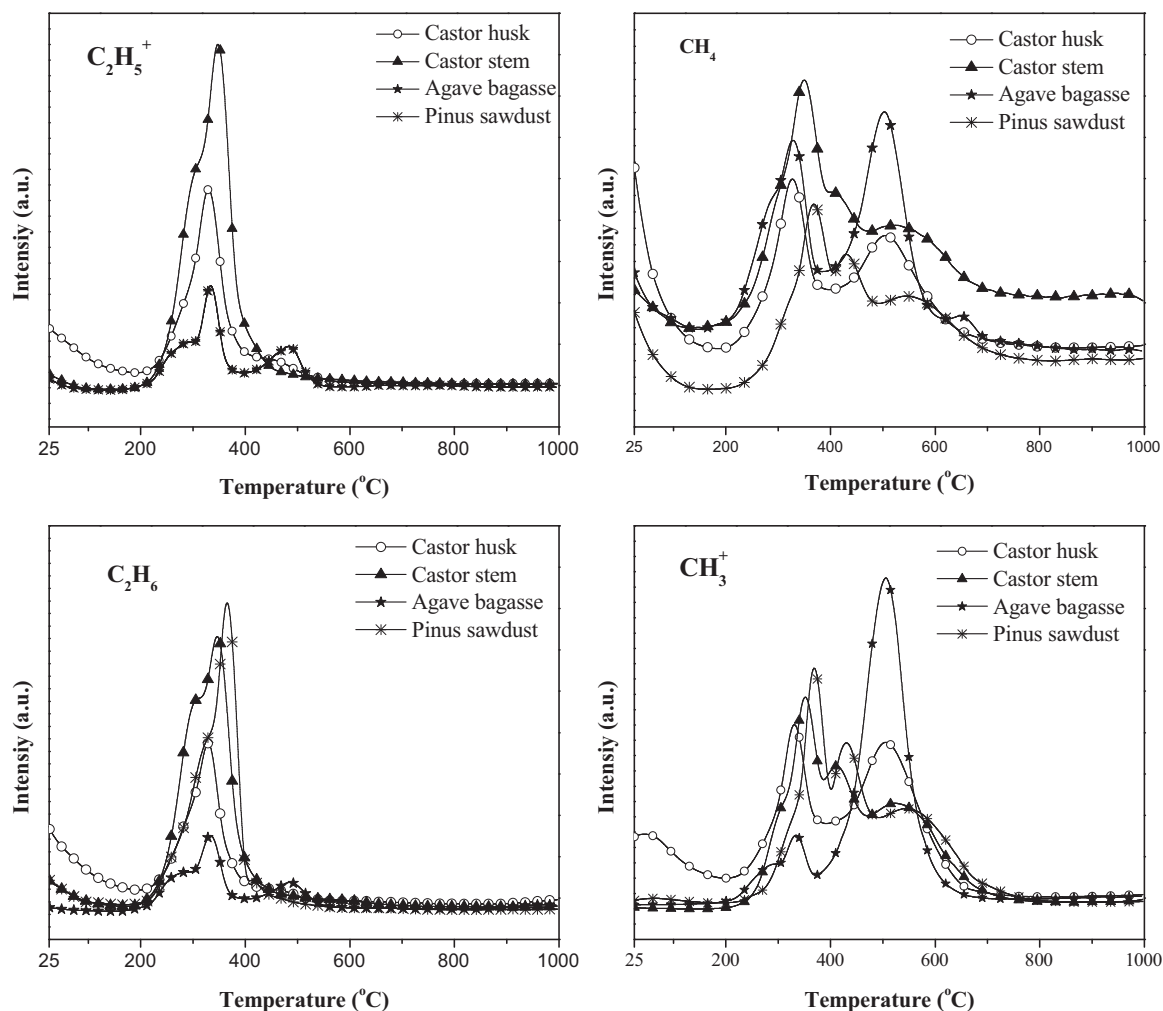
Fig. 5. Mass spectra of the pyrolysis process of Castor husk, Castor stems, *Agave* bagasse, *Pinus* sawdust for: $C_2H_5^+$, CH_4, C_2H_6 and CH_3^+.

tion stage, Castor husk, Castor stem and *Pinus* sawdust presented similar TGA profiles. On the contrary, the *Pinus* sawdust decomposition shifted to higher temperatures. The devolatilization stage for Castor husk and Castor stem occurred at low temperatures, which can be associated to their high cellulose content [34,91]. On the other hand, it was noted that the third DTG peak for Castor stem (Table 3) was the highest one followed by that of Castor husk, *Pinus* sawdust and Coffee pulp. It was observed for both Castor samples that the third DTG peak was higher than the second one, which is related to the fact that the volatile matter in both samples were burned at a lower rate and for a long time [90].

On the other hand, Coffee pulp showed a fourth peak at 592 °C (Table 3), which was associated to its high lignin content [92]. In addition, DTG curve for this sample showed the smallest and widest peaks. These findings were attributed to the lignin oxidation. Lignin presents a three-dimensional structure consisting of phenylpropane coupled with C-C or C-O-C bonds whose activity covers a wide range of temperatures [91]. Furthermore, the devolatilization stage for Coffee pulp was shifted to lower temperatures, which was associated to the presence of methoxy functional groups coming from the lignin decomposition, whereas the oxidation stage was shifted to higher temperatures. According to Kai et al. [91], the lignin is the most thermal stable component of biomass and decomposes in a wide temperature range (150–700 °C).

Finally, the residue yield of biomass combustion can be seen in Table 3. Like that observed for the pyrolysis process, it can be related to the ash content and fixed carbon (Table 1). Therefore, *Pinus* sawdust

presented the lowest yield residue (0.38 wt%), followed by Castor stem (0.76 wt%), Castor husk (7.07 wt%) and Coffee pulp (9.40 wt%).

Fig. 8 shows the DSC curves for the combustion process of *Pinus* sawdust, Coffee pulp, Castor husk and Castor stem. DSC analysis determines the heat released during the combustion process. Two exothermic regions for *Pinus* sawdust, Castor husk and Castor stem and three exothermic regions for Coffee pulp were found. The first region was associated to the release of light volatile matters which provided reactivity to the biomass fuel and the second stage was due to the combustion of fixed carbon [93]. The most prominent peak was found in the second stage.

In addition, the ignition temperature, which is the temperature at which the combustion process starts, and the burnout temperature, which is the temperature at which the combustion process finishes, were calculated for all of the samples considered in this study. Thus, Coffee pulp presented the lowest ignition temperature (152 °C), followed by Castor husk (179 °C), Castor steam (205 °C) whereas the highest ignition temperature was found for *Pinus* sawdust (225 °C). These results are in good agreement with their volatile matter content (Table 1). The burnout temperature of Coffee pulp (the highest ash content, 6.55 wt%) was also the highest one (606.5 °C). The burnout temperature of Castor husk (3.60 wt% ash content) was 490.5 °C, Finally, *Pinus* sawdust and Castor stem (with the lowest ash content, 1.30 and 1.70 wt%, respectively) yielded very close burnout temperature, 486 °C and 486.5 °C, respectively. On the other hand, the heat released during the combustion process of Castor husk was the highest one (9.98 kJ/g), followed by the Coffee pulp (9.71 kJ/g), Castor stem
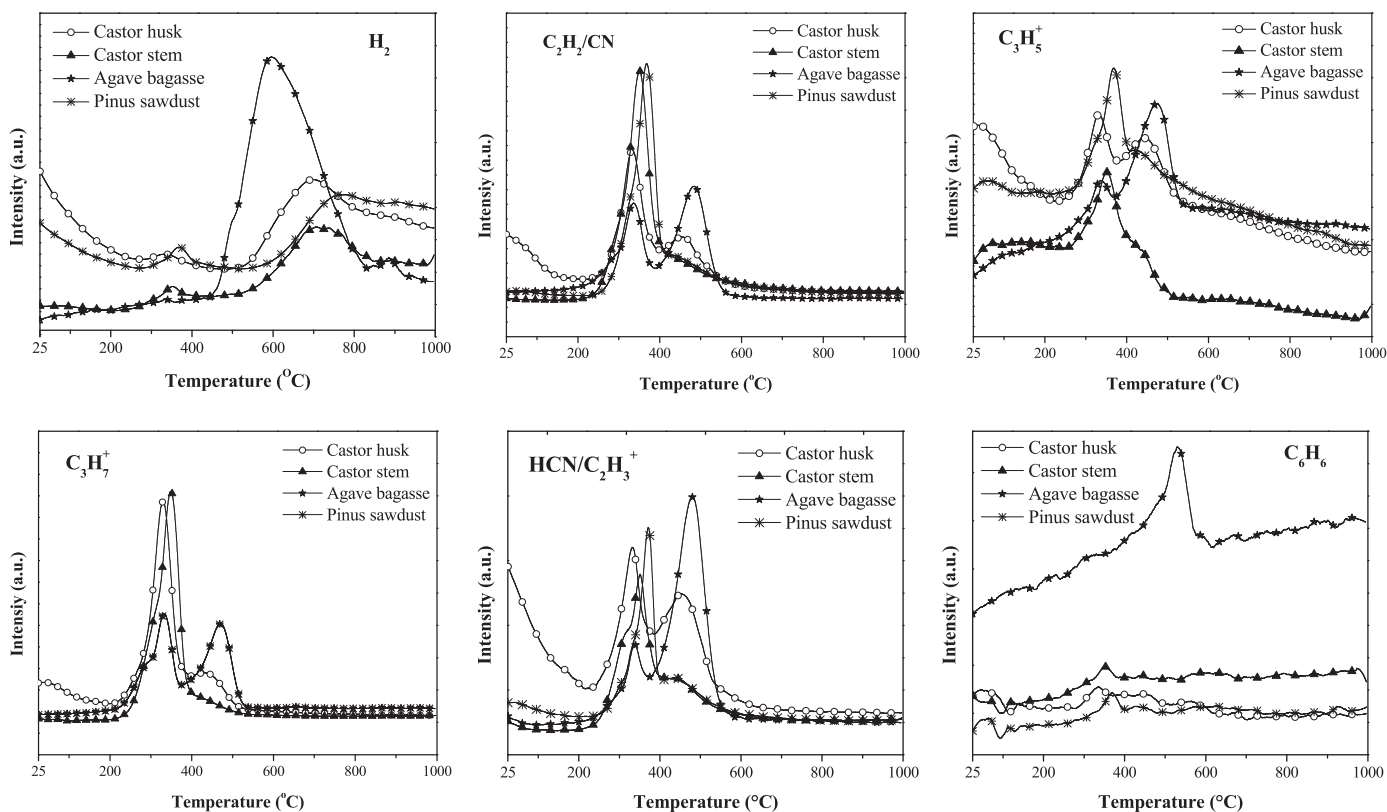
Fig. 6. Mass spectra of the pyrolysis process of Castor husk, Castor stems, *Agave* bagasse, *Pinus* sawdust for: H_2, C_2H_2/CN, $C_3H_5^+$, $C_3H_7^+$, $HCN/C_2H_3^+$ and C_6H_6.
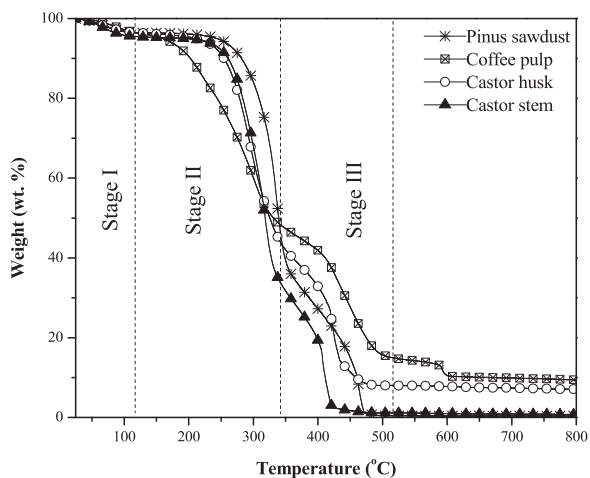

Fig. 7. TGA curves for the combustion process of: *Pinus* sawdust, Coffee pulp, Castor husk and Castor stem.
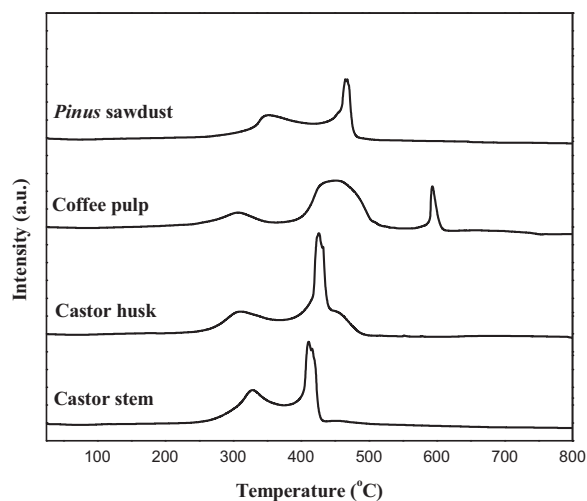

Fig. 8. DSC curves for the combustion process of: *Pinus* sawdust, Coffee pulp, Castor husk and Castor stem.

Table 3
Combustion characteristics of *Pinus* sawdust, Coffee pulp, Castor husk and Castor stems.

Biomass sample	T_{comb}[a] (°C)	T_m (°C)[b]				$(dw/dT)_{max}$ (wt%/°C)[c]				Residue yield (wt%)
		1st peak	2nd peak	3rd peak	4th peak	1st peak	2nd peak	3rd peak	4th peak	
Pinus sawdust	205	71	336	462	–	0.06	1.59	1.21	–	0.38
Coffee pulp	130	73	302	437	592	0.06	0.44	0.35	0.49	9.40
Castor husk	169	64	295	420	–	0.06	0.77	1.41	–	7.07
Castor stem	196	70	319	406	–	0.08	1.26	1.59	–	0.76

[a] Temperature at which combustion started.
[b] Temperature at which a peak in the DTG curve was observed.
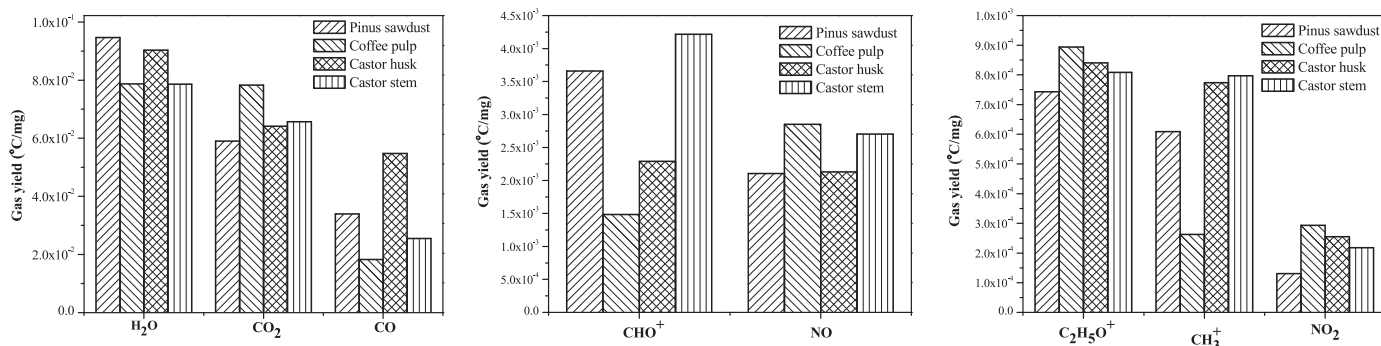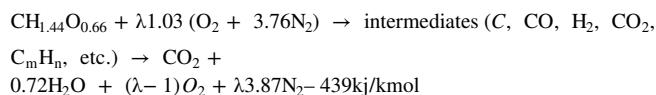[c] Maximum weight loss rate.

Fig. 9. Integrated peak areas for the combustion process of *Pinus* sawdust, Coffee pulp, Castor husk and Castor stem for: H_2O, CO_2, CO, CHO^+, NO, $C_2H_5O^+$, CH_3^+ and NO_2.

(7.08 kJ/g) whereas the lowest one was found for *Pinus* sawdust (6.44 kJ/g).

The biomass combustion reaction can be described according to the following equation:

$$CH_{1.44}O_{0.66} + \lambda 1.03 \, (O_2 + 3.76N_2) \rightarrow \text{intermediates} \, (C, \, CO, \, H_2, \, CO_2,$$
$$C_mH_n, \, \text{etc.}) \rightarrow CO_2 +$$
$$0.72H_2O + (\lambda - 1)O_2 + \lambda 3.87N_2 - 439kj/kmol$$

where $CH_{1.44}O_{0.66}$ is considered to be the composition of a typical biomass [94].

The main gas products derived from the combustion of *Pinus* sawdust, Coffee pulp, Castor husk and Castor stem were evaluated by MS analysis. Therefore, the main ions related to the gases emitted in the combustion process were detected at (m/z)=15, 18, 28, 29, 30, 44, 45 and 46, corresponding to the following compounds: CH_3^+, H_2O, CO, CHO^+, NO, CO_2, $C_2H_5O^+$ and NO_2, respectively.

The main integrated peak areas of the mass spectra of the gases coming from the combustion of *Pinus* sawdust, Coffee pulp, Castor husk and Castor stem are shown in Fig. 9. CH_3^+, H_2O, CO, CHO^+, NO, CO_2, $C_2H_5O^+$ and NO_2 were detected at the second stage (125–350 °C), when the devolatilization of biomass proceeded, and in the last stage (350–525 °C), corresponding to the oxidation of char. In addition, the maximum intensity peak for H_2O, CHO^+ and NO was observed in the devolatilization stage, whereas that for CH_3^+, CO, CO_2, $C_2H_5O^+$ and NO_2. were observed in the third stage.

The main products obtained during the combustion process of the studied biomasses were H_2O, CO_2 and CO. First of all, H_2O presented the highest intensity peak and was released in all of the stages. Regarding the first stage (25–125 °C), H_2O detected in the MS spectrum was related to the loss of moisture. The larger peak of H_2O emission was found in the devolatilization stage, which corresponded to the evolution of aliphatic OH groups [95]. Finally, the smallest one was detected in the third stage, which is related to both the formation of water during the oxidation of H_2 and the calcium carbonate decomposition [34]. On the other hand, CO and CO_2 emissions were a consequence of the combustion of fixed carbon [49]. The amount of CO_2 released might act as an indicator of the combustion efficiency as it is the main product of the direct oxidation of the char. However, CO_2 production can be catalyzed or inhibited by the formation of combustion intermediates [96]. Coffee pulp released the highest CO_2 emission which could be related to its high lignin content. On the other hand, CO was formed by the occurrence of molecular oxide complexes that rearrange afterwards [34]. In addition, the incomplete combustion of organic material can also lead to high emissions of CO and unburnt pollutants. Castor husk released the highest CO amount, which could be attributed to its incomplete combustion. Moreover, the most relevant component of this biomass is nitrogen which leads to NO_x emission (NO_2 and NO). Those products can be formed by three different reactions. Thus, thermal and prompt NO_x are formed at high temperatures from the reaction of nitrogen with air whereas fuel NO_x

are formed from nitrogen-containing fuels. Furthermore, fuel-containing nitrogen can be converted into intermediate products (HCN and NH_i), which in presence of O_2 are in turn converted into NO_x [94]. Moreover, the presence of CaO, MgO and Fe_2O_3 in the biomass can form an active bed which could catalyze the reduction of NO and N_2O. Therefore, the highest NO_x emission was found for Coffee pulp which can be related to its high nitrogen content. On the other hand, the lowest NO_x emission was observed for sample *Pinus* sawdust, with the lowest nitrogen content. In addition, the release of the CH_3^+ and CHO^+ during the first stage was due to the volatile matter decomposition whereas that observed during the second stage could be attributed to the decomposition of the solid residue [49]. The lowest amount of those products was found for Coffee pulp and the highest one was observed for Castor stem. Finally, for Coffee pulp the different products were released in the three stages but highest amount of the main released products (CO, NO, CO_2, $C_2H_5O^+$, and NO_2) was observed during the fourth stage.

On the other hand, biomass can be used at industrial scale to obtain renewable energy. There are a lot of parameters which can influence the use of biomass to obtain energy, such as: moisture content, bulk density, ash content, pollutants emission, melting point and corrosion properties. First of all, the moisture content of biomass has to be low enough. High moisture fuels burn harder and provide less useful heat per unit mass, and consequently affects the quality of combustion process [61]. Moisture content of biomass is a factor which limits the combustion process due to its effect on heating value. The combustion process is exothermic and the evaporation of water is endothermic [65]. The biomasses here studied presented a low moisture content, ranging from 1.57 to 4.27 wt% (Table 1). Another parameter affecting not only the rates of heating and drying during the combustion process but also its processing, transportation and storage is the bulk density of the biomass [61]. The biomasses reported in this study can be used in combustion processes at industrial scale since they present a density ranging from 1346 to 1726 kg/m³ (Table 1). On the other hand, the ash content in a biomass should be low if it must be used for energy purposes. Moreover, the presence of certain inorganic elements (K, Si, Cl) can cause corrosion and erosion of metals [61]. Specifically, potassium oxide can affect the melting properties of ash [61]. Low melting points of the ashes can cause serious operational problems including agglomeration, fouling, slagging and corrosion. Consequently, a biomass used for energy purposed should have a low inorganic content. Excluding *Agave* bagasse and *Opuntia* stem, the rest of biomasses presented a low ash content (Table 1). This way, *Pinus* sawdust and Coffee pulp with an ash content of 1.30 and 6.55 wt%, respectively, presented better properties to be used in combustion process at industrial scale.

3.4. Gasification process

It is known that O_2 concentration is an important factor that influences the gasification process in terms of syngas production and
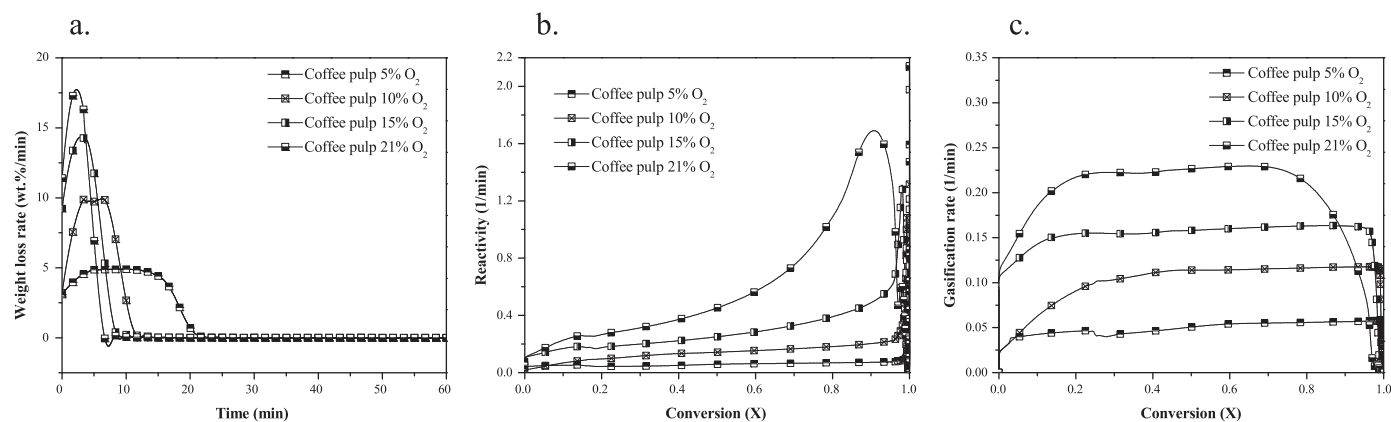
Fig. 10. Gasification process of Coffee pulp for different O_2 concentration (5, 10, 15 and 21 vol%): a. DTG curve, b. reactivity and c. gasification rate.

affects the operation costs. Therefore, it is necessary to determine the O_2 concentration leading to a cost-effective gasification for the studied biomass.

The effect of O_2 concentration (5, 10, 15 and 21 vol%) on the gasification process of Coffee pulp char was evaluated at 900 °C for 1 h (Fig. 10). DTG peaks height increased whereas their width decreased with increasing O_2 concentrations (Fig. 10a). Therefore, the smallest and the widest peak was obtained for a O_2 concentration of 5 vol%; the tallest and the narrowest peak was obtained for a O_2 concentration of 21 vol%$_2$. As expected, the higher the O_2 concentration, the higher the reactivity was. Similar results were reported by Rathnam et al. [97].

On the other hand, char conversion, reactivity and gasification rate are important parameters to characterise the gasification process. Char conversion, X, represents the weight loss fraction or mass conversion ratio, and it was calculated according to the following equation:

$$X = \frac{w_i - w_t}{w_i - w_f} \qquad (1)$$

where w_i is the initial mass of the char sample at time t_0, w_t is the mass of the char sample at time t and w_f is the final mass of the char sample [98]. Moreover, the reactivity of char was calculated by the following equation:

$$R = -\frac{1}{w} \cdot \frac{dw}{dt} = \frac{1}{1-X} \cdot \frac{dX}{dt} \qquad (2)$$

The reactivity is dependent on the temperature and gas composition and varies with the conversion degree [99]. In this work, reactivity at 50% char conversion (R_{50}) was considered to be representative of the gasification process. Thus, the gasification rate was defined as follows:

$$r = \frac{dX}{dt} \qquad (3)$$

Table 4 shows the gasification characteristics of *Opuntia* stem and Coffee pulp (for 5, 10, 15 and 21 vol% of O_2), being X_{99} the time to achieve 99% of conversion, X_{50} the time to achieve 50% of conversion and R_{50} the reactivity at 50% char conversion.

Table 4
Gasification characteristics for *Opuntia* stem and Coffee pulp (5, 10, 15 and 21 vol% O_2).

Biomass sample	Time X_{99} (min)[a]	Time X_{50} (min)[a]	R_{50} (1/min)[b]
Opuntia stem 10% O_2	10.9	2.2	0.42
Coffee pulp 5% O_2	23.3	9.3	0.11
Coffee pulp 10% O_2	12.5	5	0.24
Coffee pulp 15% O_2	11.4	3.3	0.32
Coffee pulp 21% O_2	10.9	2.5	0.45

[a] Time to achieve 99% and 50% conversion, respectively.

[b] The reactivity corresponding to 50% conversion.

Fig. 10(b, c) show the reactivity and gasification rate vs. conversion plots for the gasification of Coffee pulp at different O_2 concentration. It was observed that the reactivity increased for char conversion values higher than 0.8 [99]. Moreover, as it was above-mentioned, the reactivity increased for increasing values of O_2 concentration, thus, for Coffee pulp R_{50} increases from 0.11 min^{-1} (5 vol% O_2) to 0.45 min^1 (21 vol% O_2) (Table 4). Furthermore, Table 4 shows for the same biomass the values of the time required to get X_{99} and X_{50} at different O_2 concentration. As expected, it can be seen that the higher the O_2 concentration, the lower the values of X_{99} and X_{50} are.

Fig. 11 shows (a) the DTG curve, (b) the reactivity and (c) the gasification rate obtained from the analysis of the gasification process of *Opuntia* stem and Coffee pulp using a O_2 concentration of 10 vol% of O_2. If compared to Coffee pulp, it was observed that *Opuntia* stem decomposed faster and the yield residue was higher (Table 4). This fact can be attributed to the different composition of each biomass. According to López-González et al. and Di Blasi [99,100], the char conversion is a complex process in comparison with the devolatilization one. In addition, it is a heterogeneous process since the chemical reactions take place on the surface. The reactivity of char is influenced by three different characteristics of the biomass such as the content of inorganic matter, and its chemical structure and porosity [35,99,100]. In addition, the reactivity R_{50} of *Opuntia* stem was higher (0.42 min^{-1}) than that of the Coffee pulp (0.24 min^{-1}) (Table 4), which is related to the catalytic effect of the inorganic in nature active species present in the raw [101]. *Opuntia* stem contained a higher mineral content (39,319, 5101, 4745 and 8369 ppm of Ca, P, K and Mg, respectively) than Coffee pulp (Table 1). Finally, the yield residue obtained from *Opuntia* stem was higher (46.65%) than that obtained from Coffee pulp (17.8%), which is related to the higher ash content (15.32 wt%) and the low fixed carbon (16.33 wt%) of the former.

On the other hand, Figs. 12 and 13 shows a comparison among the SEM images of the raw *Opuntia* stem and Coffee pulp samples and their chars produced after the pyrolysis and gasification processes. It can be seen that both raw biomasses show rough surface particles with no cavities and similar particle size distribution. However, the average particles size of the pyrolytic and gasification chars coming from *Opuntia* stem was bigger than those coming from Coffee pulp. Furthermore, the resulting char particles obtained from both samples tended to lose their original structure and presented smooth surfaces [102].

Finally, the main gas products derived from the gasification of *Opuntia* stem and Coffee pulp were evaluated by means of MS analysis. The main ions related emitted in the pyrolysis process were detected at (m/z)=2, 16, 28, 29, 30, 44 and 46, corresponding to the following species: H_2, CH_4, CO, $C_2H_5^+$, NO, CO_2, and NO_2, respectively.

Figs. 14 and 15 show the main integrated peak areas of the mass spectra obtained from the gasification process of *Opuntia* stem and
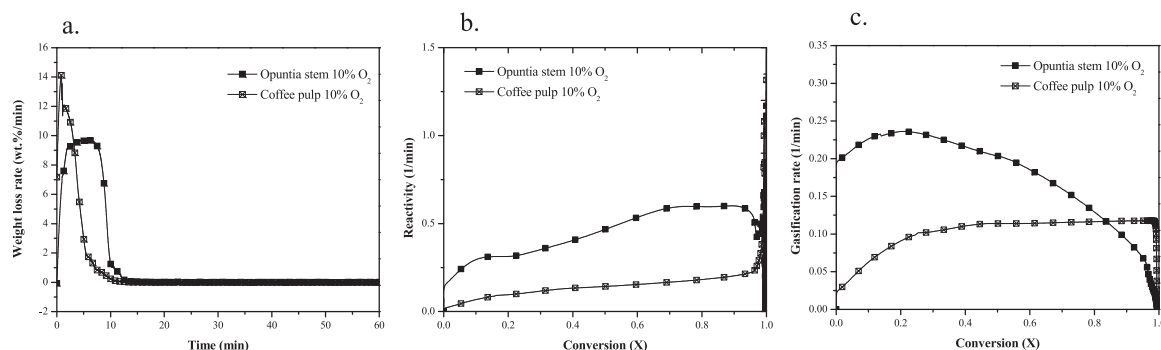
Fig. 11. Gasification process of *Opuntia* stem and Coffee pulp: a. DTG curve; b. reactivity; c. gasification rate.

Coffee pulp. Fig. 14 shows the composition and characteristic ratios of the fuel gas obtained from both biomasses. It was observed that the CO_2, CO, CH_4 and H_2 intensities obtained from Coffee pulp were higher than those obtained from *Opuntia* stem, which is related to the higher content of carbon and hydrogen in the former sample (43.33 and 5.69 wt%, respectively) than in the later (34.72 and 5.07 wt%, respectively). Also, it could be related to the high fixed carbon content in Coffee pulp (21.23 wt%) if compared to that of *Opuntia* stem (16.33 wt %) (Table 1).

In both cases, CO_2 was the predominant gas. It can be released from the following reactions: $C+O_2 \rightarrow CO_2$ and $CO+\frac{1}{2}O_2 \rightarrow CO_2$. On the other hand, the CO was the second specie most released after CO_2 and can be obtained from these reactions: $C+\frac{1}{2}O_2 \rightarrow CO$ and $C+CO_2 \rightarrow 2CO$ [103]. CH_4 was also released in high proportion from secondary reactions

such as: $C+2H_2 \rightarrow CH_4$ and $C_nO_m \rightarrow C_{n-x}H_{m-y}+H_2+CH_4+C$ [99].

Fig. 15 shows the intensity of the peaks corresponding to $C_2H_5^+$, NO and NO_2. The two latter are a consequence of the reactions conditions, which could reform volatile-N and gasify char-N, leading to the formation of nitrogen species [104].

Among all the mexican biomasses studied, *Pinus* sawdust showed the best pyrolysis behaviour because it presented the highest volatile matter (80.15 wt%) and the lowest ash (1.30 wt%) contents and led to high yield gas production, *Agave* bagasse was the less suitable biomass for pyrolysis process due to its low volatile matter (71.00 wt%) and high ash contents (11.41 wt%), resulting in a high concentration of polluted species (HCN and C_6H_6) in the exhaust. Regarding the combustion process, Castor husk resulted to be the most appropriate biomass due to its high heat released (9.98 kJ/g). However, from the
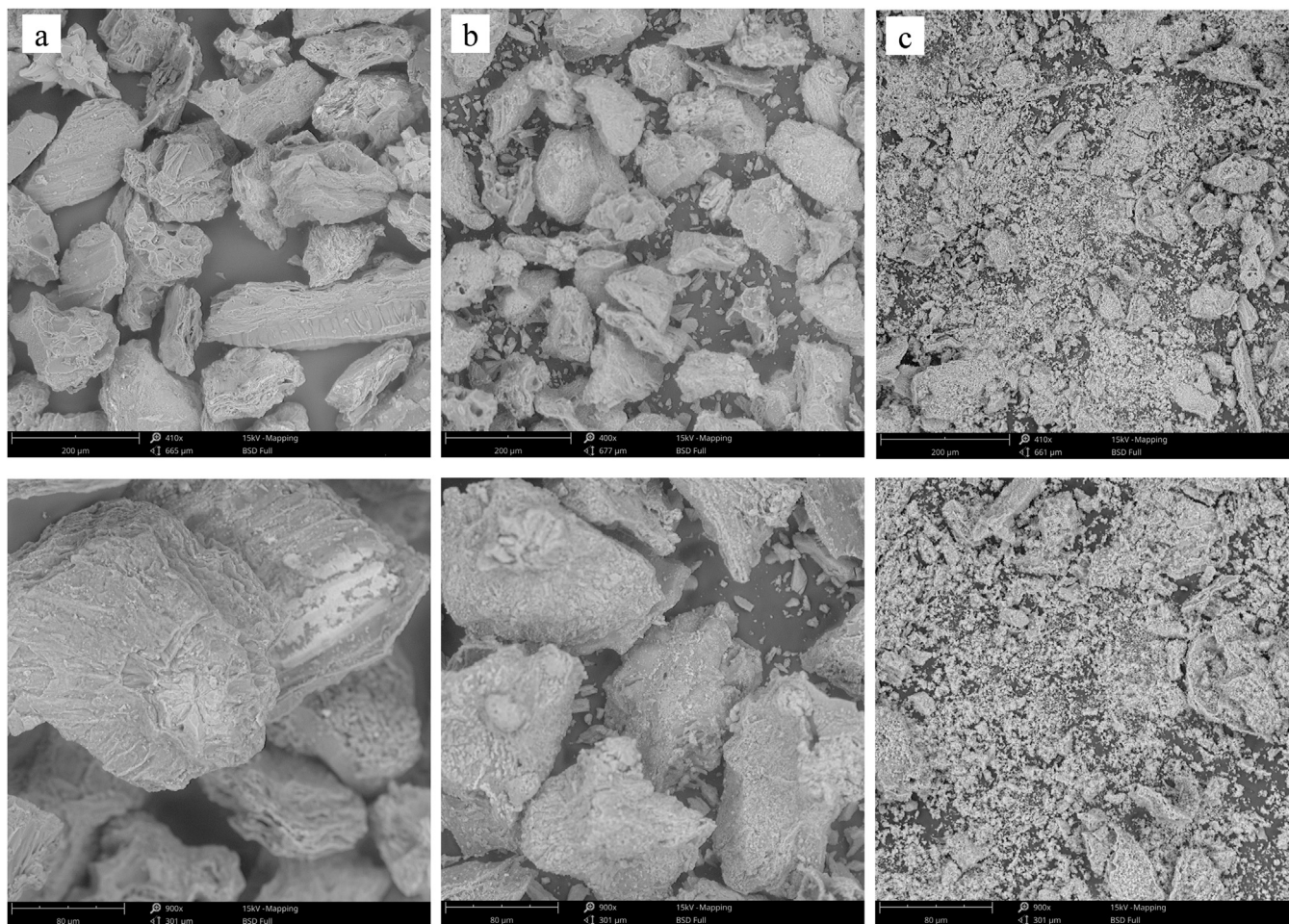

Fig. 12. SEM images showing the typical morphology of the particles in sample *Opuntia* stem collected after: a. original sample; b. pyrolysis process; c. gasification process.
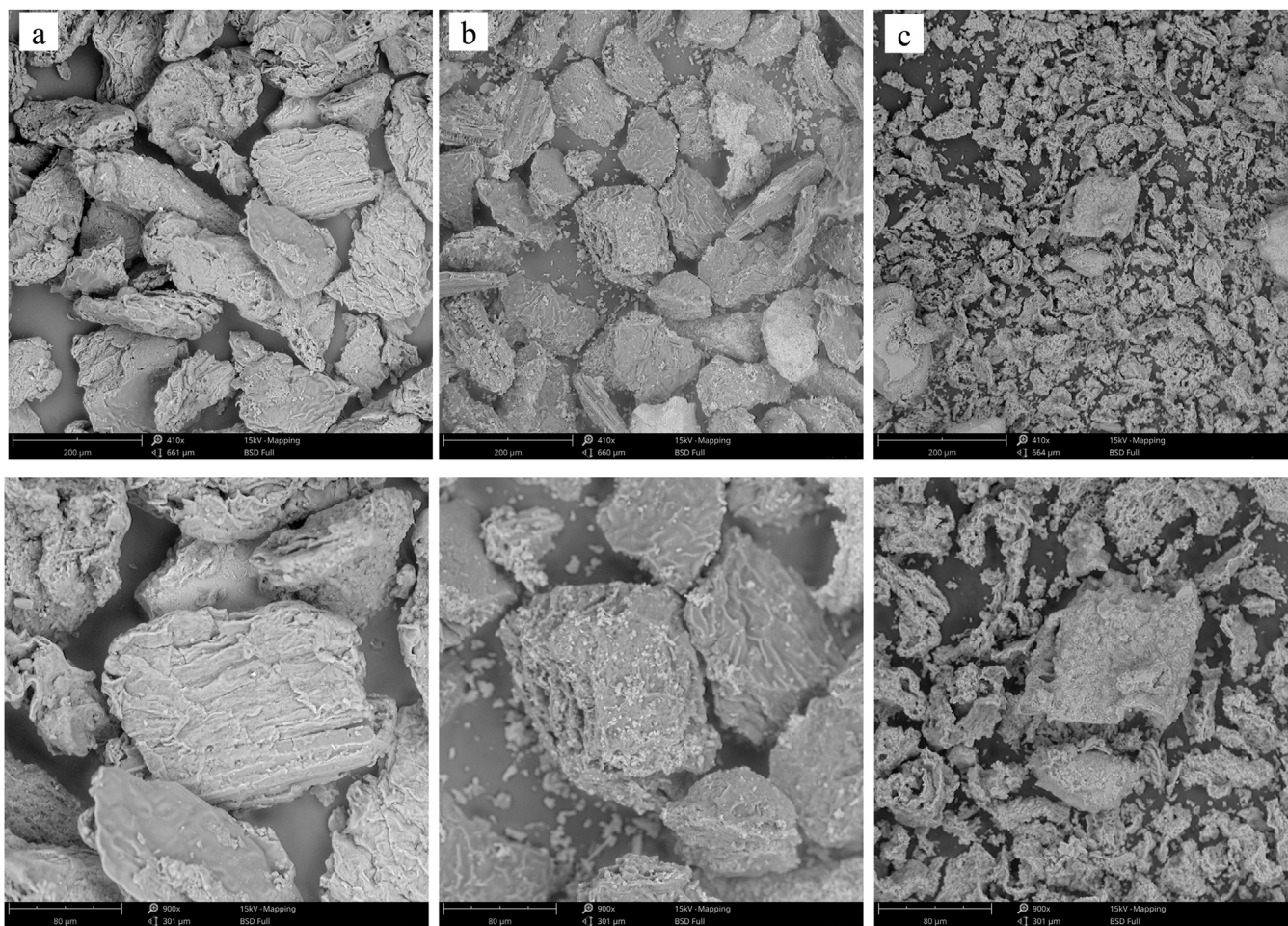
Fig. 13. SEM images showing the typical morphology of the particles in sample Coffee pulp collected after: a. original sample; b. pyrolysis process; c. gasification process.

point of view of emitted gases, the most environmental friendly biomass was *Pinus* sawdust. Finally, Coffee pulp resulted to be the most suitable biomass for gasification process, due to the quality and concentration of the gas released (H_2, CO, CH_4 and $C_2H_5^+$) during the process.

4. Conclusions

The thermal behaviour of six different types of biomass (Castor husk, Castor stem, Agave bagasse, Coffee pulp, Opuntia stem and Pinus sawdust) has been investigated via TGA-MS in order to know their potential to be valorised as a renewable energy source under different process configuration (pyrolysis, combustion and gasification).
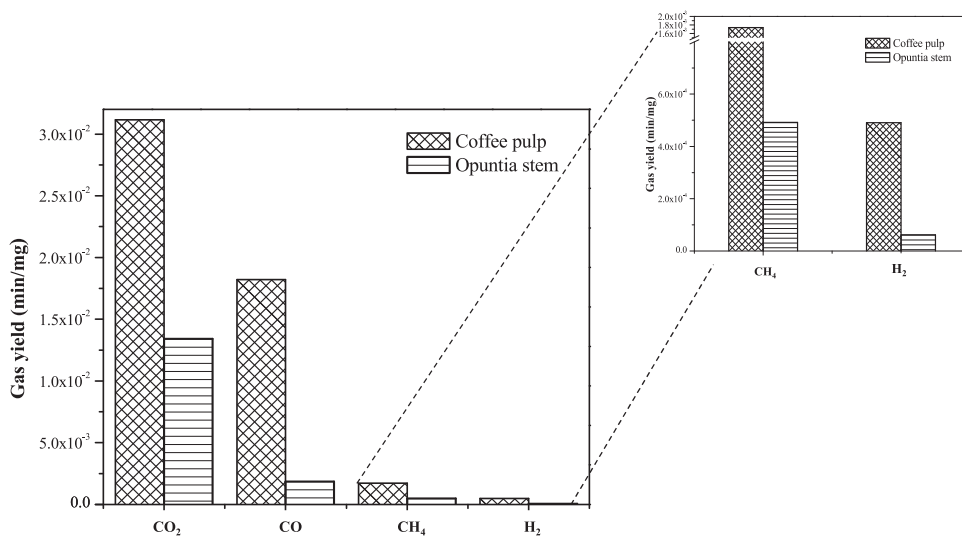

Fig. 14. Integrated peak areas for the gasification process of Coffee pulp and *Opuntia* stem for: CO_2, CO, CH_4 and H_2.
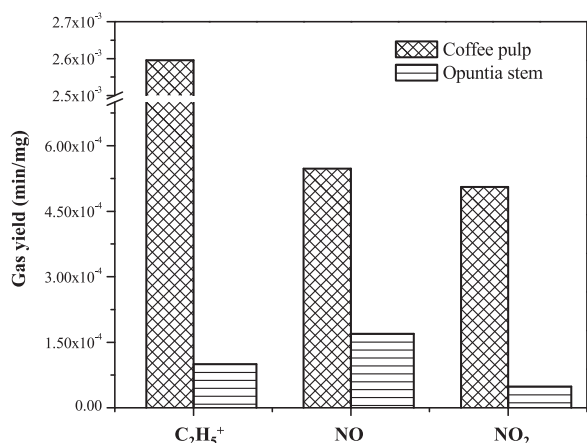
Fig. 15. Integrated peak areas for the gasification process of Coffee pulp and *Opuntia* stem for: $C_2H_5^+$, NO and NO_2.

Physical-chemical characterization of these biomasses has been used within the making decision process in order to determine the most appropriate configuration for each type of studied biomass. Based on their characteristic, Castor husk, Castor stems, *Agave* bagasse and *Pinus* sawdust were selected for pyrolysis; *Pinus* sawdust, Coffee pulp, Castor husk and Castor stem were used for combustion; and Coffee pulp and *Opuntia* stem were selected for gasification. The pyrolysis process could be defined by three different stages (dehydration, devolatilization and char formation). The temperature at which the main decomposition took place ranged from 200 to 500 °C (devolatilization stage). Particularly CH_3^+, CH_4, H_2O, C_2H_2/CN, $HCN/C_2H_3^+$, CO, $C_2H_5^+$, C_2H_6 $C_3H_5^+$, $C_3H_7^+$ and CO_2 were the main products released as a result of biomass decomposition during this stage. On the other hand, three main different stages of combustion process (dehydration, devolatilization and oxidation) were found. The last oxidation stage occurred between 350 and 525 °C, being CH_3^+, CO, CO_2, $C_2H_5O^+$ and NO_2 the main products released during this stage. The gasification process was studied at low O_2 concentration. The gasification under deficit O_2 condition was little studied and therefore an extensive research was conducted in order to determine the optimal concentration of O_2 being 10 vol% O_2 selected. Increasing oxygen concentrations favored the decomposition of biomass at shorter times. During gasification process H_2, CH_4, CO, $C_2H_5^+$, NO, CO_2 and NO_2 were detected.

Pinus sawdust was the most appropriate biomass for pyrolysis. Castor husk could be considered for combustion due to the high heat released in the process. However, *Pinus* sawdust are to be considered more suitable from the environmental point of view. Finally, Coffee pulp resulted to be the most adequate for gasification due to the amount and quality of the fuel gas produced.

Acknowledgment

References

[1] Escobar JC, Lora ES, Venturini OJ, Yáñez EE, Castillo EF, Almazan O. Biofuels: environment, technology and food security. Renew Sust Energy Rev 2009;13:1275–87.

[2] Caspeta L, Caro-Bermúdez MA, Ponce-Noyola T, Martinez A. Enzymatic hydrolysis at high-solids loadings for the conversion of agave bagasse to fuel ethanol. Appl Energy 2014;113:277–86.

[3] Okello C, Pindozzi S, Faugno S, Boccia L. Development of bioenergy technologies in Uganda: a review of progress. Renew Sust Energ Rev 2013;18:55–63.

[4] Corro G, Pal U, Bañuelos F, Rosas M. Generation of biogas from coffee-pulp and cow-dung co-digestion: infrared studies of postcombustion emissions. Energy Convers Manag 2013;74:471–81.

[5] Valdez-Vazquez I, Acevedo-Benítez JA, Hernández-Santiago C. Distribution and potential of bioenergy resources from agricultural activities in Mexico. Renew Sust Energy Rev 2010;14:2147–53.

[6] Azadi P, Inderwildi OR, Farnood R, King DA. Liquid fuels, hydrogen and chemicals from lignin: a critical review. Renew Sust Energy Rev 2013;21:506–23.

[7] Geydan TD, Melgarejo LM. Metabolismo ácido de las crasuláceas. Acta Biol Colomb 2005;10:3–16.

[8] López-González D, Avalos-Ramirez A, Giroir-Fendler A, Godbout S, Fernandez-Lopez M, Sanchez-Silva L, et al. Combustion kinetic study of woody and herbaceous crops by thermal analysis coupled to mass spectrometry. Energy 2015;90:1626–35.

[9] Yang Q, Pan X. Pretreatment of Agave americana stalk for enzymatic saccharification. Bioresour Technol 2012;126:336–40.

[10] Yang L, Lu M, Carl S, Mayer JA, Cushman JC, Tian E, et al. Biomass characterization of Agave and Opuntia as potential biofuel feedstocks. Biomass Bioenergy 2015;76:43–53.

[11] Esquivel P, Jiménez VM. Functional properties of coffee and coffee by-products. Food Res Int 2012;46:488–95.

[12] Rattan S, Parande AK, Nagaraju VD, Ghiwari GK. A comprehensive review on utilization of wastewater from coffee processing. Environ Sci Pollut R 2015;22:6461–72.

[13] Menezes EGT, Do Carmo JR, Menezes AGT, Alves JGLF, Pimenta CJ, Queiroz F. Use of different extracts of coffee pulp for the production of bioethanol. Appl Biochem Biotechnol 2013;169:673–87.

[14] Bonilla-Hermosa VA, Duarte WF, Schwan RF. Utilization of coffee by-products obtained from semi-washed process for production of value-added compounds. Bioresour Technol 2014;166:142–50.

[15] Orozco AL, Pérez MI, Guevara O, Rodríguez J, Hernández M, González-Vila FJ, et al. Biotechnological enhancement of coffee pulp residues by solid-state fermentation with Streptomyces. Py-GC/MS analysis. J Anal Appl Pyrolysis 2008;81:247–52.

[16] Murthy PS, Madhava Naidu M. Sustainable management of coffee industry by-products and value addition – a review. Resour Conserv Recycl 2012;66:45–58.

[17] Gurram R, Al-Shannag M, Knapp S, Das T, Singsaas E, Alkasrawi M. Technical possibilities of bioethanol production from coffee pulp: a renewable feedstock. Clean Technol Environ Policy 2016;18:269–78.

[18] Pandey A, Soccol CR, Nigam P, Brand D, Mohan R, Roussos S. Biotechnological potential of coffee pulp and coffee husk for bioprocesses. Biochem Eng J 2000;6:153–62.

[19] Hughes SR, López-Núñez JC, Jones MA, Moser BR, Cox EJ, Lindquist M, et al. Sustainable conversion of coffee and other crop wastes to biofuels and bioproducts using coupled biochemical and thermochemical processes in a multi-stage biorefinery concept. Appl Microbiol Biotechnol 2014;98:8413–31.

[20] Wright JA. Utilization of pinus patula: an annotated bibliography. Oxford Forestry Institute, Department of Plant Sciences, University of Oxford; 1994.

[21] Barnes DJ, Baldwin BS, Braasch DA. Degradation of ricin in castor seed meal by temperature and chemical treatment. Ind Corp Prod 2009;29:509–15.

[22] Bateni H, Karimi K, Zamani A, Benakashani F. Castor plant for biodiesel, biogas, and ethanol production with a biorefinery processing perspective. Appl Energy 2014;136:14–22.

[23] Lima RLS, Severino LS, Sampaio LR, Sofiatti V, Gomes JA, Beltrão NEM. Blends of castor meal and castor husks for optimized use as organic fertilizer. Ind Corp Prod 2011;33:364–8.

[24] Herculano PN, Porto TS, Moreira KA, Pinto GAS, Souza-Motta CM, Porto ALF. Cellulase production by Aspergillus japonicus URM5620 using waste from castor bean (Ricinus communis L.) under solid-state fermentation. Appl Biochem Biotechnol 2011;165:1057–67.

[25] Madeira JV, Macedo JA, Macedo GA. Detoxification of castor bean residues and the simultaneous production of tannase and phytase by solid-state fermentation using Paecilomyces variotii. Bioresour Technol 2011;102:7343–8.

[26] Andrade MM, Barbosa AM, Bofinger MR, Dekker RFH, Messias JM, Guedes CLB, et al. Lipase production by Botryosphaeria ribis EC-01 on soybean and castorbean meals: optimization, immobilization, and application for biodiesel production. Appl Biochem Biotechnol 2013;170:1792–806.

[27] Melo WC, Dos Santos AS, Santa Anna LMM, Pereira JrN. Acid and enzymatic hydrolysis of the residue from Castor Bean (Ricinus communis L.) oil extraction for ethanol production: detoxification and biodiesel process integration. J Braz Chem Soc 2008;19:418–25.

[28] Alves EEN, Souza CDF, Inoue KRA, Leite TDS. Potential of production of biogas from the castor bean (Ricinus communis L.) cake. American Society of Agricultural and Biological Engineers Annual International Meeting 2010, ASABE 2010; 2010. p. 3829–34.

[29] Raheem A, Sivasangar S, Wan Azlina WAKG, Taufiq Yap YH, Danquah MK, Harun R. Thermogravimetric study of Chlorella vulgaris for syngas production. Algal Res 2015;12:52–9.

[30] Chen Y-C, Chen W-H, Lin B-J, Chang J-S, Ong HC. Impact of torrefaction on the composition, structure and reactivity of a microalga residue. Appl Energy 2016;181:110–9.

[31] Soreanu G. Insights into siloxane removal from biogas in biotrickling filters via process mapping-based analysis. Chemosphere 2016;146:539–46.

[32] Demirbas A. Biofuels securing the planet's future energy needs. Energy Convers Manag 2009;50:2239–49.

[33] Shen J, Igathinathane C, Yu M, Pothula AK. Biomass pyrolysis and combustion integral and differential reaction heats with temperatures using thermogravimetric analysis/differential scanning calorimetry. Bioresour Technol 2015;185:89–98.

[34] López-González D, Fernandez-Lopez M, Valverde JL, Sanchez-Silva L.

Thermogravimetric-mass spectrometric analysis on combustion of lignocellulosic biomass. Bioresour Technol 2013;143:562–74.

[35] Jayaraman K, Gökalp I. Pyrolysis, combustion and gasification characteristics of miscanthus and sewage sludge. Energy Convers Manag 2015;89:83–91.

[36] Aranda G, Grootjes AJ, Van Der Meijden CM, Van Der Drift A, Gupta DF, Sonde RR, et al. Conversion of high-ash coal under steam and CO_2 gasification conditions. Fuel Process Technol 2016;141:16–30.

[37] Siriwardane R, Riley J, Tian H, Richards G. Chemical looping coal gasification with calcium ferrite and barium ferrite via solid-solid reactions. Appl Energy 2016;165:952–66.

[38] Wang F, Zeng X, Wang Y, Su H, Yu J, Xu G. Non-isothermal coal char gasification with CO_2 in a micro fluidized bed reaction analyzer and a thermogravimetric analyzer. Fuel 2016;164:403–9.

[39] Zhang Y, Zheng Y, Yang M, Song Y. Effect of fuel origin on synergy during co-gasification of biomass and coal in CO_2. Bioresour Technol 2016;200:789–94.

[40] Mueller A, Haustein HD, Stoesser P, Kreitzberg T, Kneer R, Kolb T. Gasification kinetics of biomass- and fossil-based fuels: comparison study using fluidized bed and thermogravimetric analysis. Energy Fuels 2015;29:6717–23.

[41] Martin AR, Martins MA, Da Silva ORRF , Mattoso LHC. Studies on the thermal properties of sisal fiber and its constituents. Thermochim Acta 2010;506:14–9.

[42] Methacanon P, Weerawatsophon U, Sumransin N, Prahsarn C, Bergado DT. Properties and potential application of the selected natural fibers as limited life geotextiles. Carbohydr Polym 2010;82:1090–6.

[43] Satyanarayana KG, Flores-Sahagun THS, Dos Santos LP, Dos Santos J, Mazzaro I, Mikowski A. Characterization of blue agave bagasse fibers of Mexico. Compos Part A: Appl Sci Manuf 2013;45:153–61.

[44] Perez-Pimienta JA, Lopez-Ortega MG, Chavez-Carvayar JA, Varanasi P, Stavila V, Cheng G, et al. Characterization of agave bagasse as a function ofionic liquid pretreatment. Biomass- Bioenerg 2015;75:180–8.

[45] Chávez-Guerrero L, Hinojosa M. Bagasse from the mezcal industry as an alternative renewable energy produced in arid lands. Fuel 2010;89:4049–52.

[46] Nieto-Delgado C, Terrones M, Rangel-Mendez JR. Development of highly micro-porous activated carbon from the alcoholic beverage industry organic by-products. Biomass Bioenerg 2011;35:103–12.

[47] González A, Penedo M, Mauris E, Fernández-Berridi MJ, Irusta L, Iruin J. Pyrolysis analysis of different Cuban natural fibres by TGA and GC/FTIR. Biomass Bioenerg 2010;34:1573–7.

[48] Song Y, Tahmasebi A, Yu J. Co-pyrolysis of pine sawdust and lignite in a thermogravimetric analyzer and a fixed-bed reactor. Bioresour Technol 2014;174:204–11.

[49] Sanchez-Silva L, López-González D, Garcia-Minguillan AM, Valverde JL. Pyrolysis, combustion and gasification characteristics of Nannochloropsis gaditana microalgae. Bioresour Technol 2013;130:321–31.

[50] Wang X, Zhao B, Yang X. Co-pyrolysis of microalgae and sewage sludge: biocrude assessment and char yield prediction. Energy Convers Manag 2016;117:326–34.

[51] Polat S, Apaydin-Varol E, Pütün AE. Thermal decomposition behavior of tobacco stem Part I: TGA–FTIR–MS analysis. Energy Sources Part A: Recovery Util Environ Eff 2016;38:3065–72.

[52] Sellin N, Krohl DR, Marangoni C, Souza O. Oxidative fast pyrolysis of banana leaves in fluidized bed reactor. Renew Energy 2016;96:56–64.

[53] Cantrell K, Martin J, Ro K. Application of thermogravimetric analysis for the proximate analysis of livestock wastes; 2010.

[54] Wu H, Hanna MA, Jones DD. Thermogravimetric characterization of dairy manure as pyrolysis and combustion feedstocks. Waste Manag Res 2012;30:1066–71.

[55] Fernandez-Lopez M, Puig-Gamero M, Lopez-Gonzalez D, Avalos-Ramirez A, Valverde J, Sanchez-Silva L. Life cycle assessment of swine and dairy manure: pyrolysis and combustion processes. Bioresour Technol 2015;182:184–92.

[56] Fernandez-Lopez M, López-González D, Puig-Gamero M, Valverde JL, Sanchez-Silva L. CO_2 gasification of dairy and swine manure: a life cycle assessment approach. Renew Energy 2016;95:552–60.

[57] Liu S-C, Tsai W-T. Thermochemical characteristics of dairy manure and its derived biochars from a fixed-bed pyrolysis. Int J Green Energy 2016;13:963–8.

[58] Al-Qodah Z, Shawabkah R. Production and characterization of granular activated carbon from activated sludge. Braz J Chem Eng 2009;26:127–36.

[59] Yahya MA, Al-Qodah Z, Ngah CWZCW, Hashim MA. Preparation and character-ization of activated carbon from desiccated coconut residue by potassium hydroxide. Asian J Chem 2015;27:2331–6.

[60] Yahya MA, Al-Qodah Z, Ngah CWZ. Agricultural bio-waste materials as potential sustainable precursors used for activated carbon production: a review. Renew Sustain Energy Rev 2015;46:218–35.

[61] Werther J, Saenger M, Hartge EU, Ogada T, Siagi Z. Combustion of agricultural residues. Prog Energy Combust Sci 2000;26:1–27.

[62] Sanchez-Silva L, López-González D, Villaseñor J, Sánchez P, Valverde JL. Thermogravimetric-mass spectrometric analysis of lignocellulosic and marine biomass pyrolysis. Bioresour Technol 2012;109:163–72.

[63] Protásio TP, Bufalino L, Tonoli GHD, Guimarães Junior MG, Trugilho PF, Mendes LM. Brazilian lignocellulosic wastes for bioenergy production: Characterization and comparison with fossil fuels. BioResources 2013;8:1166–85.

[64] Garivait S, Chaiyo U, Patumsawad S, Deakhuntod J. Fuel characteristics of agricultural residues in Thailand. Energy Sources Part A: Recovery Util Environ Eff 2013;35:826–30.

[65] Jenkins BM, Baxter LL, Miles TR, Jr, Miles TR. Combustion properties of biomass. Fuel Process Technol 1998;54:17–46.

[66] Obernberger I, Thek G. Physical characterisation and chemical composition of densified biomass fuels with regard to their combustion behaviour. Biomass

Bioenerg 2004;27:653–69.

[67] Moore A, Park S, Segura C, Carrier M. Fast pyrolysis of lignin-coated radiata pine. J Anal Appl Pyrolysis 2015;115:203–13.

[68] Can M. Equilibrium, kinetics and process design of acid yellow 132 adsorption onto red pine sawdust. Water Sci Technol 2015;71:1901–11.

[69] Barra BN, Santos SF, Bergo PVA, Alves C, Ghavami K, Savastano H. Residual sisal fibers treated by methane cold plasma discharge for potential application in cement based material. Ind Corp Prod 2015;77:691–702.

[70] Zborowska M, Stachowiak-Wencek A, Nowaczyk-Organista M, Waliszewska B, Pradzyński W. Analysis of photodegradation process of Pinus sylvestris L. wood after treatment with acid and alkaline buffers and light irradiation. BioResources 2015;10:2057–66.

[71] Liñán-Montes A, De La Parra-Arciniega SM, Garza-González MT, García-Reyes RB, Soto-Regalado E, Cerino-Córdova FJ. Characterization and thermal analysis of agave bagasse and malt spent grain. J Therm Anal Calorim 2014;115:751–8.

[72] Yang H, Yan R, Chen H, Lee DH, Zheng C. Characteristics of hemicellulose, cellulose and lignin pyrolysis. Fuel 2007;86:1781–8.

[73] Yuan T, Tahmasebi A, Yu J. Comparative study on pyrolysis of lignocellulosic and algal biomass using a thermogravimetric and a fixed-bed reactor. Bioresour Technol 2015;175:333–41.

[74] Zabeti M, Sai Sankar Gupta KB, Raman G, Lefferts L, Schallmoser S, Lercher JA, et al. Aliphatic hydrocarbons from lignocellulose by pyrolysis over. ChemCatChem 2015;7:3386–96.

[75] Santos NAV, Magriotis ZM, Saczk AA, Fássio GTA, Vieira SS. Kinetic study of pyrolysis of castor beans (Ricinus communis L.) Presscake: an alternative use for solid waste arising from the biodiesel production. Energy Fuels 2015;29:2351–7.

[76] Ounas A, Aboulkas A, El harfi K, Bacaoui A, Yaacoubi A. Pyrolysis of olive residue and sugar cane bagasse: non-isothermal thermogravimetric kinetic analysis. Bioresour Technol 2011;102:11234–8.

[77] Velazquez-Jimenez LH, Rangel-Mendez JR. Chemical and thermogravimetric analyses of raw and saturated agave bagasse main fractions with Cd(II), Pb(II), and Zn(II) ions: adsorption mechanisms. Ind Eng Chem Res 2014;53:8332–8.

[78] Paraschiv M, Kuncser R, Tazerout M, Prisecaru T. New energy value chain through pyrolysis of hospital plastic waste. Appl Therm Eng 2015;87:424–33.

[79] Hewitt F, Rhebat DE, Witkowski A, Hull TR. An experimental and numerical model for the release of acetone from decomposing EVA containing aluminium, magnesium or calcium hydroxide fire retardants. Polym Degrad Stab 2016;127:65–78.

[80] Li S, Ma X. Catalytic characteristics of the pyrolysis of lignite over oil shale chars. Appl Therm Eng 2016;106:865–74.

[81] Seo DK, Park SS, Hwang J, Yu T-U. Study of the pyrolysis of biomass using thermo-gravimetric analysis (TGA) and concentration measurements of the evolved species. J Anal Appl Pyrolysis 2010;89:66–73.

[82] Cortés AM, Bridgwater AV. Kinetic study of the pyrolysis of miscanthus and its acid hydrolysis residue by thermogravimetric analysis. Fuel Process Technol 2015;138:184–93.

[83] Zhang J, Zhong Z, Zhang B, Xue Z, Guo F, Wang J. Prediction of kinetic parameters of biomass pyrolysis based on the optimal mixture design method. Clean Technol Environ Policy 2016;18:1621–9.

[84] Asadieraghi M, Wan Daud WMA. In-situ catalytic upgrading of biomass pyrolysis vapor: using a cascade system of various catalysts in a multi-zone fixed bed reactor. Energy Convers Manag 2015;101:151–63.

[85] Sun S, Tian H, Zhao Y, Sun R, Zhou H. Experimental and numerical study of biomass flash pyrolysis in an entrained flow reactor. Bioresour Technol 2010;101:3678–84.

[86] Várhegyi G, Czégény Z, Jakab E, McAdam K, Liu C. Tobacco pyrolysis. Kinetic evaluation of thermogravimetric-mass spectrometric experiments. J Anal Appl Pyrolysis 2009;86:310–22.

[87] López-González D, Puig-Gamero M, Acién FG, García-Cuadra F, Valverde JL, Sanchez-Silva L. Energetic, economic and environmental assessment of the pyrolysis and combustion of microalgae and their oils. Renew Sust Energ Rev 2015;51:1752–70.

[88] Cruz G, Crnkovic PM. Investigation into the kinetic behavior of biomass combustion under N2/O2 and CO_2/O2 atmospheres. J Therm Anal Calorim 2016;123:1003–11.

[89] Pécora AAB, Ávila I, Lira CS, Cruz G, Crnkovic PM. Prediction of the combustion process in fluidized bed based on physical-chemical properties of biomass particles and their hydrodynamic behaviors. Fuel Process Technol 2014;124:188–97.

[90] Gil MV, Oulego P, Casal MD, Pevida C, Pis JJ, Rubiera F. Mechanical durability and combustion characteristics of pellets from biomass blends. Bioresour Technol 2010;101:8859–67.

[91] Kai X, Yang T, Huang Y, Sun Y, He Y, Li R. The effect of biomass components on the co-combustion characteristics of biomass with coal. In: Proceedings of the 2011 2nd international conference on digital manufacturing and automation, ICDMA 2011; 2011. p. 1274–78.

[92] Rambo MKD, Alexandre GP, Rambo MCD, Alves AR, Garcia WT, Baruque E. Characterization of biomasses from the north and northeast regions of Brazil for processes in biorefineries. Food Sci Technol 2015;35:605–11.

[93] Kok MV, Özgür E. Thermal analysis and kinetics of biomass samples. Fuel Process Technol 2013;106:739–43.

[94] Nussbaumer T. Combustion and co-combustion of biomass: Fundamentals, technologies, and primary measures for emission reduction. Energy Fuels 2003;17:1510–21.

[95] Jakab E, Till F, Várhegyi G. Thermogravimetric-mass spectrometric study on the low temperature oxidation of coals. Fuel Process Technol 1991;28:221–38.

[96] Shen D, Hu J, Xiao R, Zhang H, Li S, Gu S. Online evolved gas analysis by Thermogravimetric-Mass Spectroscopy for thermal decomposition of biomass and its components under different atmospheres: Part I. Lignin. Bioresour Technol 2013;130:449–56.

[97] Rathnam RK, Elliott LK, Wall TF, Liu Y, Moghtaderi B. Differences in reactivity of pulverised coal in air (O2/N2) and oxy-fuel (O2/CO2) conditions. Fuel Process Technol 2009;90:797–802.

[98] Gil MV, Riaza J, Álvarez L, Pevida C, Rubiera F. Biomass devolatilization at high temperature under N2 and CO_2: Char morphology and reactivity. Energy 2015;91:655–62.

[99] López-González D, Fernandez-Lopez M, Valverde JL, Sanchez-Silva L. Gasification of lignocellulosic biomass char obtained from pyrolysis: kinetic and evolved gas analyses. Energy 2014;71:456–67.

[100] Di Blasi C. Combustion and gasification rates of lignocellulosic chars. Prog Energy Combust Sci 2009;35:121–40.

[101] Marquez-Montesinos F, Cordero T, Rodríguez-Mirasol J, Rodríguez JJ. CO_2 and steam gasification of a grapefruit skin char. Fuel 2002;81:423–9.

[102] Gonzalo-Tirado C, Jiménez S, Ballester J. Gasification of a pulverized sub-bituminous coal in CO_2 at atmospheric pressure in an entrained flow reactor. Combust Flame 2012;159:385–95.

[103] Rodriguéz C, Gordillo G. Sugar cane bagasse gasification using air-steam for partial oxidation and N2 as carrier gas. In: Proceedings of the ASME Turbo Expo; 2012. p. 701-709.

[104] Ren Q, Zhao C, Wu X, Liang C, Chen X, Shen J, et al. Formation of NOx precursors during wheat straw pyrolysis and gasification with O2 and CO_2. Fuel 2010;89:1064–9.